Archives of Materials Science and Engineering

Volume 40
Issue 1
November 2009
Pages 27-32

International Scientific Journal
published monthly by the
World Academy of Materials
and Manufacturing Engineering

Microstructural and thermal analysis of Cu-Ni-Sn-Zn alloys by means of SEM and DSC techniques

G. Wnuk, M. Zielińska*
Department of Materials Science, Rzeszow University of Technology, Rzeszów, Poland
* Corresponding author: E-mail address: gwnuk@prz.edu.pl

Received 23.08.2009; published in revised form 01.11.2009

ABSTRACT

Purpose: The urgent need to find new, non toxic, high temperature solders caused the abundance of research on multicomponent systems, so as to find new materials that could substitute lead-containing solders.

Design/methodology/approach: In the paper Cu-Ni-Sn-Zn alloys were studied by differential scanning calorymetry (DSC) in argon atmosphere using a heating rate of 10 $Kmin^{-1}$ and a cooling rate of 15 $Kmin^{-1}$. There were determined heat effects and start and finish temperature of phase transitions. Each sample was heated and cooled twice. At the second run, Zn concentration was smaller (as Zn is a volatile component).

Findings: Zn influence on phase transformations was established. For the second run, when Zn activity is smaller, heats and temperature of transformations are higher.

Research limitations/implications: These experimental results, combined with other thermodynamic properties of the studied alloy, enable phase diagram calculation in the frame of the COST action MP0602.

Practical implications: Phase diagrams of the studied alloys allow finding appropriate solder materials.

Originality/value: The paper presents an influence of zinc on temperature and heats of transformations in Cu-Ni-Sn-Zn alloys and the microstructure of these alloys.

Keywords: Cu-Ni-Sn-Zn alloys; DSC technique; Scanning electron microscopy

Reference to this paper should be given in the following way:

G. Wnuk, M. Zielińska, Microstructural and thermal analysis of Cu-Ni-Sn-Zn alloys by means of SEM and DSC techniques, Archives of Materials Science and Engineering 40/1 (2009) 27-32.

MATERIALS

1. Introduction

Most Pb-free solders are Sn-based alloys with addition of low melting metals (such as Zn) or metals forming eutecticts or peritectics with Sn (such as Cu). Copper and nickel are common substrate materials. Therefore, systems containing these elements need to be evaluated thoroughly. [1, 2].

Binary and ternary alloys constituting the investigated quaternary system were studied [3-8], but for the Cu-Ni-Sn-Zn system, there were only some thermodynamic measurements performed by means of an equilibrium saturation method [9].

When the binary and ternary subsystems are known, thermodynamic calculation provides an extremely useful tool for obtaining quantitative information about higher-order (ternary, quaternary, *etc.*) systems. Ternary assessments can be combined for extrapolation to a higher component system. The calculated phase equilibria data should reproduce experimental data within the limits of experimental accuracy [10]. Although experimental determination of higher-order systems is time consuming, some experimental data are necessary to compare the calculations with.

In this paper, calorimetric and microscopic studies of the Cu-Ni-Sn-Zn system are presented. They are a part of an overall examination of the Cu-Ni-X-Y systems (X, Y = Sn, Bi, Zn, Ti) in relation to development of new lead-free solders in the frame of the COST action MP0602.

2. Experimental procedure

The investigated alloys were prepared by melting nickel, copper and tin of high purity (99.999 mass per cent) in a vacuum furnace and saturating them by vapour zinc at 1373K for 2 hours under reduced argon pressure [8] until the state of equilibrium was reached. The chemical composition of the prepared samples is given in Figure1 and Table 1, alloy 1-6. The compositions of alloys were determined by weighing (the accuracy of weighing was 10^{-4} g) and a spectroscopic method (plasma spectrometer ULTIMA 2 HORRIBAJOBINYVON, accuracy 0.0001). The zinc concentration in the studied samples resulted from the thermodynamic equilibrium in the studied Cu-Ni-Sn-Zn alloys.

The DSC [11] measurements of all the samples were carried out on a differential scanning calorimeter [12] Setaram SetSys Evolution 12 under the following conditions: flowing argon atmosphere 50 ml/min, samples masses about 50 mg, temperature range from 300 K to 1500 K. The heating rate was 10 $Kmin^{-1}$ and the cooling rate was 15 $Kmin^{-1}$. Calibration of the apparatus was made by using the melting points of In, Sn, Zn, Al, Ag and Au and cooling and heating rates 10 and 15 $Kmin^{-1}$. The calibration procedures were performed for both cooling and heating respectively.

As during the experiment the zinc content in the alloy was decreasing, due to its evaporation, Zn concentration was determined after each run by the weighting and spectroscopic methods. There were obtained liquidus (T_{liq}) and solidus (T_{sol}) temperatures (Figs. 2, 3 and 4) and estimated enthalpies of melting ΔH_m (Table 1) of the analyzed alloys on the basis of DSC curves. Temperature of transitions was taken from the extrapolated onset on cooling.

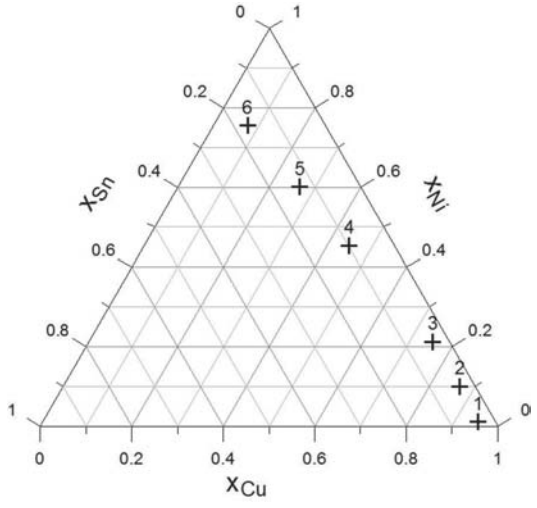

Fig. 1. Quasi-ternary diagram of Cu-Ni-(Sn, Zn) alloys

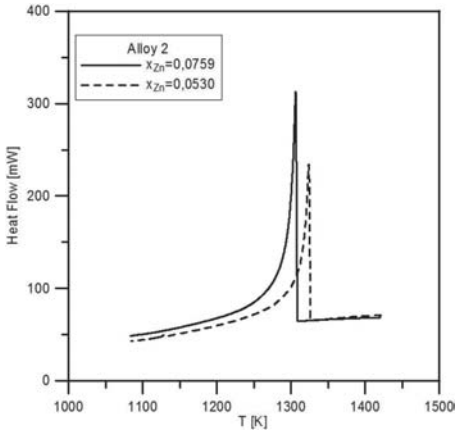

Fig. 2. Continuous cooling DSC curves obtained at 15 K/min for the alloy no 2

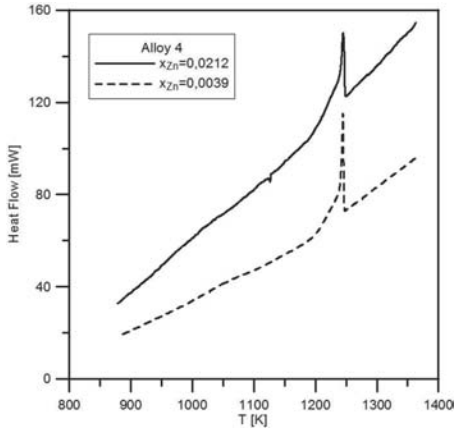

Fig. 3. Continuous cooling DSC curves obtained at 15 K/min for the alloy no 4

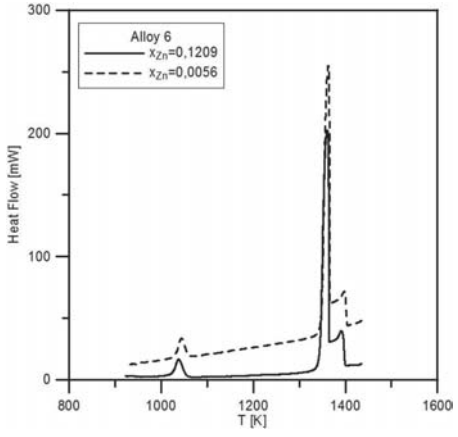

Fig. 4. Continuous cooling DSC curves obtained at 15 K/min for the alloy no 6

Microstructure investigations of the alloys before and after DSC measurements were performed by the use of a scanning electron microscope (SEM) HITACHI S-3400N equipped with an energy–dispersive spectroscope (EDS) [13-15].

3. Results and discussion

From DSC curves, temperature of onsets and ends of crystallization of the investigated alloys were obtained. Figures 2-4 present the DSC curves for alloys number 2, 4 and 6. The table 1 shows the characteristic temperatures and estimated values of ΔH_m of all alloys (1-6, Table 1) obtained from DSC curves. Alloys with high concentration of copper (0.83 and 0.66 mole fraction) with composition 1 and 2 crystallized at the constant temperature of 1288 and 1308 K. The shape of DSC curves of these alloys remains that for the pure metals (Fig. 2). For the second run, which is for alloys containing smaller amount of zinc, the liquidus temperature is higher and enthalpy of melting is bigger (Table 1).

The DSC curves of alloys of compositions no 3-5 (Table 1), with higher nickel concentration, have characteristic bend like for an alloy no 4 (Fig. 3). The crystallization process of these alloys occurs in the range of temperature 1413 (alloy no 5) and 1146 K (alloy no 3). The liquidus and solidus temperature increases because of higher concentration of nickel. For the second run, the melting temperature is higher and solidus temperature does not change significantly (Table 1).

For the alloy no 6 (Table 1) three peaks on a DSC curve were observed (Fig. 4). That means that the crystallization process takes place in three stages.
The temperature range of crystallization increases significantly and is in the range from 1400 K to 1068 K.

As zinc is a volatile element, it evaporates and its concentration changes during heating and cooling (see Table 1, runs 1 and 2). The loss of zinc depends on the thermodynamic properties of the investigated alloys, especially on interaction parameters. Zinc activity in the alloys is described by the Wagner equation:

$$\ln \gamma_{Zn} = \ln \gamma^0_{Zn} + \varepsilon^{Zn}_{Zn} x_{Zn} + \varepsilon^{Ni}_{Zn} x_{Ni} + \varepsilon^{Sn}_{Zn} x_{Sn}$$

where γ^0_{Zn} is the activity coefficient of Zn in Cu- Zn at $x_{Zn} \to 0$, $\varepsilon^{Zn}_{Zn} = (\partial \ln \gamma_{Zn} / \partial x_{Zn})$ is the interaction parameter of Zn in Cu-Zn at $x_{Zn} \to 0$,
$\varepsilon^{Ni}_{Zn} = (\partial \ln \gamma_{Zn} / \partial x_{Ni})$ is the interaction parameter of Ni in Cu-Ni-Sn-Zn at $x_{Zn} \to 0$, $x_{Ni} \to 0$,
$x_{Sn} \to 0$ and $\varepsilon^{Sn}_{Zn} = (\partial \ln \gamma_{Zn} / \partial xSn)$ is the interaction parameter of Sn in Cu-Ni-Sn-Zn at $x_{Zn} \to 0$, $x_{Sn} \to 0$, $x_{Ni} \to 0$
with parameters calculated by Romanowska *et. all*. [9]:

$$\ln \gamma_{Zn} = -1.2 + 0.53 x_{Zn} - 1.64 x_{Ni} + 4.06 x_{Sn}$$

The element, for which the interaction parameter is higher, causes increase in Zn activity, and loss of Zn increases. Therefore, when the elements content for higher interaction parameter increases, loss of the volatile component increases as well. In the investigated alloys, the loss of Zn is higher for alloys containing more Sn.

Table 1.
Chemical compositions of investigated alloys (x_{Cu}, x_{Ni}, x_{Sn}, x_{zn}) and corresponding liquidus and solidus temperatures and melting enthalpies

Alloy	x_{Cu}	x_{Ni}	x_{Sn}	x_{Zn}	T_{liq} [K]	T_{sol} [K]	ΔH_m [J/g]
1	0.830	0.009	0.033	0.129			
1-st run	0.923	0.010	0.037	0.031	1288	1288	140
2-nd run	0.944	0.010	0.037	0.008	1299	1299	150
2	0.663	0.076	0.025	0.236			
1-st run	0.802	0.092	0.030	0.076	1308	1308	130
2-nd run	0.822	0.094	0.031	0.053	1326	1326	140
3	0.589	0.166	0.028	0.217			
1-st run	0.654	0.185	0.031	0.131	1354	1146	140
2-nd run	0.719	0.203	0.0339	0.044	1384	1155	180
4	0.351	0.353	0.077	0.219			
1-st run	0.440	0.443	0.097	0.021	1392	1250	170
2-nd run	0.448	0.450	0.098	0.004	1407	1247	180
5	0.206	0.463	0.102	0.229			
1-st run	0.246	0.553	0.122	0.079	1405	1312	160
2-nd run	0.266	0.598	0.132	0.004	1413	1312	190
6	0.061	0.604	0.135	0.200			
1-st run	0.067	0.664	0.148	0.121	1400	1068	180
2-nd run	0.076	0.751	0.168	0.006	1405	1066	220

a)

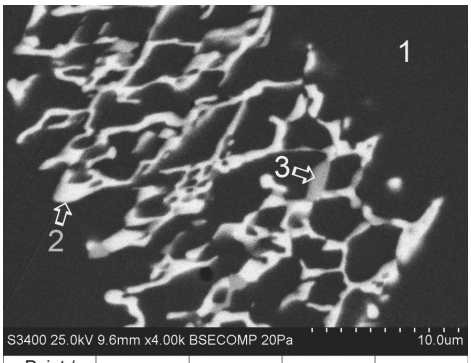

Point / Atom %	Cu	Ni	Sn	Zn
1	67	6	3	24
2	43	20	25	11
3	61	7	16	16

b)

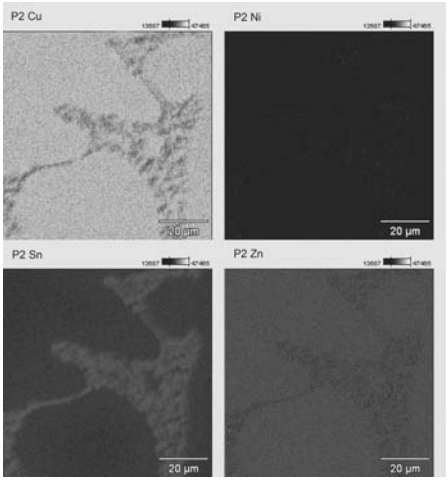

c)

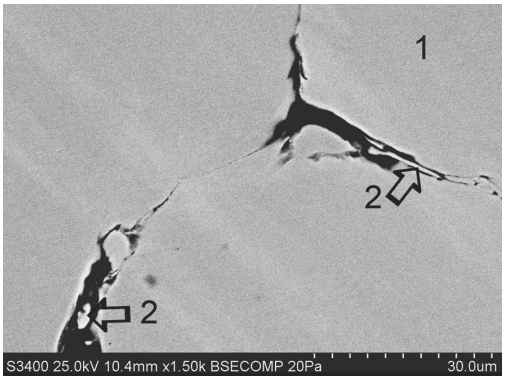

Point / Atom %	Cu	Ni	Sn	Zn
1	84	10	3	3
2	83	9	4	4

Fig. 5. SEM micrographs of alloy no 2: a) before calorimetric run, b) X-ray mapping results, c) after calorimetric run

a)

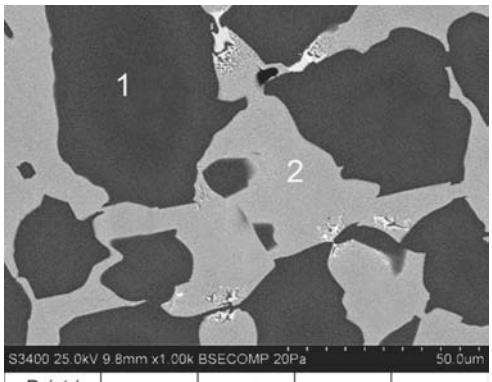

Point / Atom %	Cu	Ni	Sn	Zn
1	30	41	3	25
2	26	39	19	16

b)

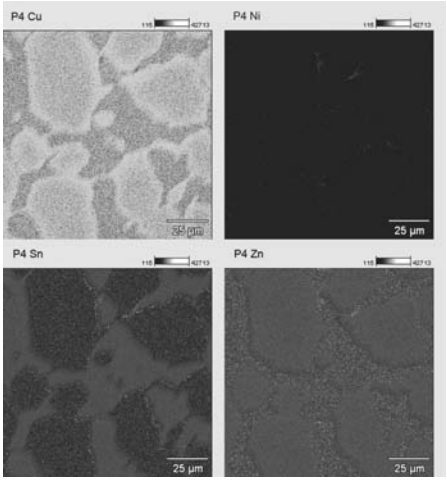

c)

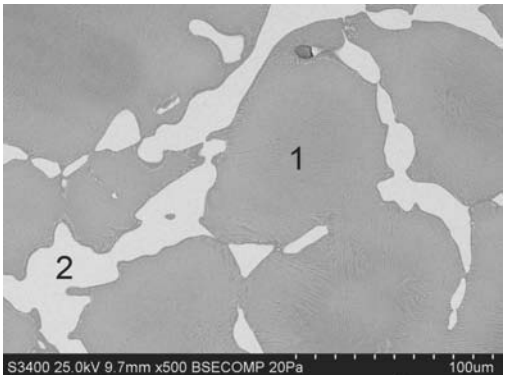

Point / Atom %	Cu	Ni	Sn	Zn
1	46	47	7	not detected
2	25	50	25	

Fig. 6. SEM micrographs of alloy no 4: a) before calorimetric run, b) X-ray mapping results, c) after calorimetric run

a)

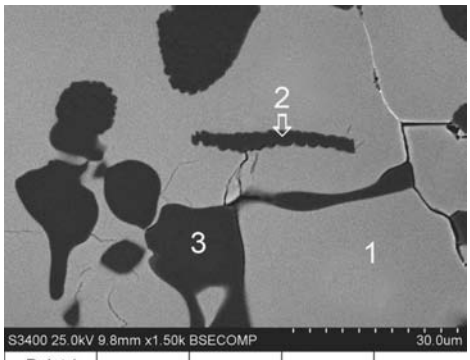

Point / Atom %	Cu	Ni	Sn	Zn
1	3	59	17	21
2	1	66	6	27
3	-	69	8	23

b)

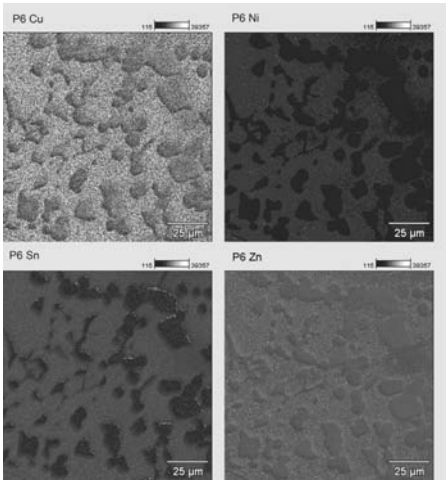

c)

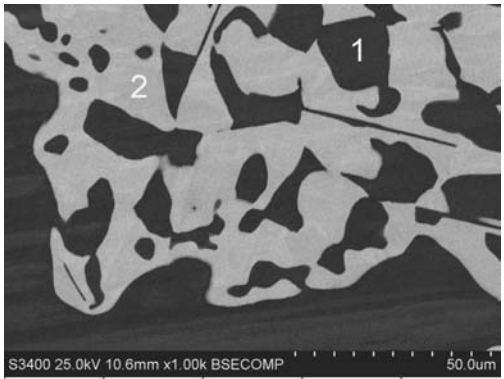

Point / Atom %	Cu	Ni	Sn	Zn
1	14	76	10	not detected
2	18	61	22	

Fig. 7. SEM micrographs of alloy no 6: a) before calorimetric run, b) X-ray mapping results, c) after calorimetric run

Microstructures and distributions of elements in the investigated alloys before the calorimetric runs are presented in Figures 5a, b (alloy no 2), in Figures 6a, b (alloy no 4) and Figures 7a, b (alloy no 6), while Figures 5c, 6c, 7c present microstructures of the alloys no 2, 4 and 6 after the second calorimetric run.

Before calorimetric run there are three phases in alloy no 2 (Figs. 5a, b). After the second run, the number of phases and their compositions change. There are two phases with very close chemical composition: the first one is the matrix and the second one is precipitations at the grain boundaries (Fig. 5c).There are visible black spaces (empty ones) at the grain boundaries. Probably, during metallographic preparation, phases that precipitated at the grain boundaries were crumbled away.

For the alloy number 4, only two phases are observed. The first phase is rich with zinc and the second with tin (Figs. 6a, b). The microstructure of the alloy no 4 changes after the second calorimetric run are made. Zinc atoms were not detected in either phase. This is due to decrease in zinc concentration in the alloy because of its evaporation.

The microstructure of alloy no 6 consists of three phases: the matrix rich with nickel, zinc and tin and two types of precipitations with very close chemical compositions but of different shapes. The precipitations which contain some copper have wrinkled surfaces, whereas the surface of phases without copper is smooth (Figs. 7a, 7b). The calorimetric annealing of the alloy no. 6 results in decrease in a number of phases (Fig. 7c).

4. Conclusions

Heat effects and the temperatures of the phase transitions start and finish were determined in Cu-Ni-Sn-Zn alloys. As zinc is a volatile component, composition of alloys changes during the calorimetric experiment. For alloys of higher tin content, the loss of zinc is bigger than for alloys of higher nickel content. This fact results from the thermodynamic properties of the Cu-Ni-Sn-Zn alloy and values of interaction parameters.

Zinc evaporation causes changes in microstructure. The number of phases reduces and chemical compositions of phases change.

Liquidus and solidus temperatures as well as enthalpies of melting determined by DSC technique will be used in thermodynamic description of the Cu-Ni-Sn-Zn system according to the CALPHAD method in the frame of the COST Action MP0602.

Acknowledgements

This work was sponsored by the Polish Ministry of Science and Higher Education, Grant no N N507 44 3834.

References

[1] T. Sasaki, M. Tanaka, Y. Ohno, Intermetallics compound formation between lead-free solders (Sn) and Cu or Ni electrodes, Materials Letters 55/10 (2007) 2093-2095.

[2] G. Niewielski, D. Kuc, Structure of the copper under controlled deformation path conditions, Archives of Materials Science and Engineering 36/1 (2009) 20-27.
[3] A. Jansson, Thermodynamic evaluation of Zn-Ni system.TRITA-MAC-0340, Materials Research Centre, Royal Institute of Technology, Stockholm, 1987.
[4] G.P. Vassilev, T. Gomez-Acebo, J.C. Tedenac, Thermodynamic optimization of the Ni-Zn system, Journal of Phase Equilibria 21 (2000) 287-301.
[5] I. Ansara, A.T. Dinsdale, M.H. Rand, COST 507-Thermochemical Database for Light Metal Alloys vol. 2, European Communities, Belgium, 1998.
[6] J. Miettinen, Thermodynamic description of the Cu-Ni-Sn system at the Cu-Ni side, Computer Coupling of Phase Diagrams and Thermochemistry 27 (2003) 263-274.
[7] C. Chou, S.Chen, Phase equilibria in the Sn-Zn-Cu ternary system, Acta Materialia 54 (2006) 2393-2400.
[8] J. Miettinen, Thermodynamic description of the Cu-Ni-Sn system at the Cu-Ni side, Computer Coupling of Phase Diagrams and Thermochemistry 27 (2003) 309-318.
[9] J. Romanowska, G. Wnuk, P. Romanowski, Experimental Study on Thermodynamics of the Cu-Ni-Sn-Zn system, Archives of Metallurgy and Materials 53/4 (2008) 1107-1110.
[10] U.R. Kattner, C. Handwerker, Calculation of Phase Equilibria in Candidate Solder Alloys, Z. Metalkd. 92/7 (2001) 740-746.
[11] A. Concustell, M. Zielińska, A. Revesz, L.K. Varga, S. Surniach, M.D. Baro, Thermal characterization of Cu60ZrxTi40-x metallic glasses (x=15, 20, 22, 25, 30), Intermetallics 12 (2004) 1063-1067.
[12] W. Zielenkiewicz, Calorymetry, Institute of Physical Chemistry of the Polish Academy of Sciences, 2008.
[13] M. Zielińska, K. Kubiak, M. Sieniawski, Surface modification, microstructure and mechanical properties of investment cast superalloy, Journal of Achievements in Materials and Manufacturing Engineering 35/1 (2009) 55-62.
[14] G. Mrówka-Nowotnik, Damage mechanism in AlSi1MgMn alloy, Archives of Materials Science and Engineering 29/2 (2008) 93-96.
[15] B.H. Kim, J.J. Jeon, K.C. Park, B.G. Park, Y.H. Park, I.M. Park, Microstructural characterization and mechanical properties of Mg-xSn-Al-Zn alloys, Archives of Materials Science and Engineering 30/2 (2008) 93-96.